



Published in final edited form as:

J Phys Chem B. 2018 February 15; 122(6): 1771–1780. doi:10.1021/acs.jpcc.7b11370.

Two-Dimensional Spectroscopy Is Being Used to Address Core Scientific Questions in Biology and Materials Science

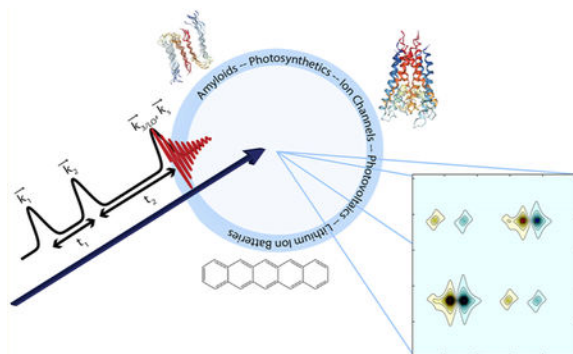
Megan K. Petti[†], Justin P. Lomont[†], Michał Maj[†], and Martin T. Zanni^{*}

Department of Chemistry, University of Wisconsin–Madison, Madison, Wisconsin 53706, United States

Abstract

Two-dimensional spectroscopy is a powerful tool for extracting structural and dynamic information from a wide range of chemical systems. We provide a brief overview of the ways in which two-dimensional visible and infrared spectroscopies are being applied to elucidate fundamental details of important processes in biological and materials science. The topics covered include amyloid proteins, photosynthetic complexes, ion channels, photovoltaics, batteries, as well as a variety of promising new methods in two-dimensional spectroscopy.

Graphical Abstract



INTRODUCTION

When answering scientific questions, chemists look for answers based on a molecular understanding. We want to learn how different ligands impact the efficiency of a catalyst, how a hydrogen bond stabilizes protein structure, or how different ion packing in crystal lattices influences the properties of a material. In essence, we want to know about how changes at a molecular level impact a system in terms of its structure and dynamics, and thus ultimately its function.

^{*}Corresponding Author zanni@chem.wisc.edu.

[†]M.K.P., J.P.L., and M.M. contributed equally to this work.

The authors declare the following competing financial interest(s): Martin Zanni is co-owner of PhaseTech Spectroscopy, Inc., which sells mid-IR and visible pulse shapers and 2D spectrometers.

There are many tools to investigate these changes, but over the past 20 years, two-dimensional (2D) spectroscopy has emerged as an optimal way to collect both structural and dynamic information. Briefly, 2D spectroscopy measures the nonlinear third order response function and can be considered as a frequency-resolved pump–probe experiment. Figure 1 depicts a pulse sequence used to obtain a two-dimensional spectrum. The time delay (population time, t_2) between the pump and probe pulses can be changed to monitor the dynamics of the system. 2D spectra can be obtained in the frequency or time domain. Differences in 2D spectroscopies include the wavelength of light used, phase-matching geometry, and phase control.^{1–3}

No matter the details of the experimental setup, 2D spectroscopy's main advantages are its structural sensitivity and intrinsic time resolution. 2D spectroscopy provides structural sensitivity due to the coupling between characteristic modes and cross-peaks.^{4,5} The nonlinear scaling of the intensity with transition dipole strength provides better resolution of neighboring peaks than conventional linear methods.^{6,7} The dynamics of structures and the chemical environment can be obtained by analyzing the 2D line shapes of diagonal peaks and cross-peak dynamics.^{1–5} 2D spectroscopy can also be used to probe nonequilibrium processes (transient 2D spectroscopy) and structures by triggering a chemical change.⁴ Most importantly, 2D spectroscopy has the time resolution to resolve structures on a variety of disparate time scales.

Beyond the chemical information that can be obtained from 2D spectra, the technique can be applied to a variety of systems. From transmembrane proteins to photovoltaic materials, both 2D infrared spectroscopy (2D IR) and 2D electronic spectroscopy (2D ES) have been used. This Mini-Review Article provides a brief overview of some biological and materials systems that 2D spectroscopy has investigated in recent years to answer fundamental questions about the structure and dynamics of these systems.

STRUCTURAL INFORMATION AND AGGREGATION KINETICS OF AMYLOID FIBRILS

More than 20 human diseases, including Alzheimer's, Parkinson's, and type II diabetes, are associated with the misfolding of proteins into β -sheet-rich amyloid fibrils. The formation mechanism and final structure of the amyloid fibrils are of importance for understanding these diseases and how to prevent them. 2D IR is especially equipped to monitor the spectroscopic changes of amyloid proteins during the aggregation process due to its intrinsic fast time resolution and nonlinear scaling of intensity with transition dipole strength, allowing for structural and mechanistic information to be obtained.

Most amyloid fibrils have multiple proposed structures determined from solid state NMR, X-ray crystallography, or electron crystallography. To gain residue-specific information, isotope labeling has been used as a probe of structure with linear IR techniques as well as 2D IR. Isotope labeling can shift the frequency of an individual residue, providing a site-specific probe of secondary structure.⁸ While isotope labeling is used in linear IR, it is most advantageous in 2D IR studies of excitonically delocalized systems due to the nonlinear scaling of the intensity with transition dipole strength. For 2D IR, the intensity is

proportional to μ^4 as compared to linear IR intensities that are proportional to μ^2 . This allows for easier detection of the site-specific probe. Simulations of 2D IR spectra have also been used to determine the spectroscopic features of parallel and antiparallel β -sheets to aid in peak assignment of experimental spectra.^{9,10}

2D IR has helped to inform the final fibril structure of amyloid proteins by using isotope labeling to elucidate residue-specific information.⁸ Such a technique was used by Wang et al.¹¹ to confirm a fibril structure of human islet amyloid polypeptide (hIAPP),¹² a peptide that is found in plaques on the islet cells of type II diabetes patients.^{13,14} Line width analysis of the 2D IR spectrum of hIAPP provided evidence of structural heterogeneity within the fibrils.¹⁵ Effects of post-translational modifications on hIAPP have also been studied by 2D IR. Deamidation of asparagine and glutamine was shown to disrupt both the N-terminal and C-terminal β -sheets of the final hIAPP fibril.¹⁶ 2D IR has not only been used to examine the final fibril state of hIAPP but has also provided insight on the aggregation mechanism by investigating the kinetics. In the past, ThT and linear IR have been used to monitor the kinetics of amyloid fibrils. Studying kinetics with 2D IR was made possible with pulse shaping and has been shown to be equivalent to ThT kinetics and better than linear IR.¹⁷ By isotope labeling specific residues and monitoring the amide I transition of hIAPP over the course of aggregation, a mechanism was determined that involves a transient β -sheet forming during the lag phase of hIAPP aggregation.^{18–20} Figure 2 is an example of 2D IR spectra taken at different times in the hIAPP aggregation process. As the peptides change from a monomeric to fibril form, the diagonal peaks in the 2D IR spectra change from a characteristic random-coil peak (1645 cm^{-1}) to amyloid β -sheet (1620 cm^{-1}). The isotope labeled frequency is red-shifted from the amyloid β -sheet, providing site-specific information.

Besides hIAPP, 2D IR has been used to provide structural information on other amyloid proteins associated with neurological diseases. A combination of 2D IR and isotope labeling provided evidence that the fibril structure of amyloid- β_{1-40} ($A\beta_{1-40}$) contains parallel in-register sheets, as predicted by Petkova et al.^{21,22} The same techniques were used to determine that, within the $A\beta_{1-40}$ fibrils, channels of water can form between the two parallel sheets.²³ Simulations of 2D IR spectra have been used to show that chirality-sensitive pulse configurations can be used to detect differences in $A\beta_{1-42}$ monomers.²⁴ These calculations determined that chirality-induced 2D IR has the resolution to discern a small difference in structure that cannot be obtained from other techniques, such as NMR.

α -Synuclein (α S) aggregation is hypothesized to lead to neuronal cell death associated with Parkinson's disease. A combination of 2D IR and AFM has provided evidence that α S forms antiparallel β -sheets in its fibril form, and that this final fibril structure is dependent on the ionic strength of the environment.²⁵ α S is known to have an acetylated N-terminus in its physiological state that is proposed to influence the function and aggregation of the peptide into amyloid fibrils. Recently, it has been shown that the acetylated N-terminus has little effect on the binding of α S to membranes but that it does affect the aggregation. 2D IR was used to show that N-terminal acetylation α S causes changes to the secondary structure of the final fibril as compared to wild-type α S.²⁶ Amyloid fibrils of a model polyglutamine (polyQ) sequence (associated with Huntington's disease) have also been studied by 2D IR,

suggesting a structure in which each monomer within the fibril forms an antiparallel hairpin in which two strands contribute to a single β -sheet, creating an overall β -turn structure.²⁷ 2D IR has also been used to identify amyloid β -sheet structure in cataracts of porcine lens.²⁸

QUANTUM COHERENCE OF ENERGY TRANSFER IN PHOTOSYNTHETIC SYSTEMS

2D spectroscopy has provided insight into electron transfer processes in photosynthetic systems by obtaining direct evidence for quantum coherence. Usually, the energy transfer mechanism associated with photosynthetic complexes is described in a semiclassical regime, where excited state populations “hop” along discrete energy levels.^{29,30} However, these dynamics have also been theorized to involve oscillatory populations of donors and acceptors.³¹ Quantum coherence is defined as a superposition of states that introduces correlations between the wave function amplitudes at different sites, which is important in photosynthetic complexes. The coherence accounts for the quantum-mechanical influences between states that affect how the dynamics of the energy transfer process evolves with time.

2D ES can probe this coherence by looking at the cross-peaks of two coupled states as a function of the population time. If there is coherence between two coupled states, the cross-peak will oscillate as a function of population time. The amplitude and shapes of these cross-peaks will contain beating signals at a frequency corresponding to the difference in energy of the two states.³² When applied to photosynthetic systems, this coherence is evidence of delocalization of the excitation between antenna and receptor complexes due to the strong electronic coupling in these systems.^{33–35} Delocalizing the excitation allows for effective energy transfer to span multiple molecules.^{33–35} Quantum coherence has been observed using 2D ES in different photosynthetic systems including the Fenna–Matthew–Olson bacteriochlorophyll a protein,^{36,37} bacteriopheophytin and its accessory bacteriochlorophyll in the purple bacteria reaction center,³⁸ bacteriophytochromes RpBphP2 and PaBphP,³⁹ and the photosynthetic centers associated with oxygen-evolving complex photosystem II.⁴⁰ However, the importance of long-lived coherence in photo-synthetic systems is still disputed.⁴¹

More recently, the focus has turned to mapping the energy transfer in photosystems to better understand the influence of quantum coherence. By using 2D ES, the excitation-energy flow of the entire photosynthetic system of green sulfur bacteria was mapped.⁴² Simulations of how the laser bandwidth convolutes these coherence energy mappings have also been made to better identify quantum coherence.⁴³ Further modeling and simulation has been done to explain observed long-lived coherence⁴⁴ and how quantum coherence influences the quantum yield of light harvesting complexes.⁴⁵ Besides photosynthetic systems, 2D ES has also been used to observe quantum coherence in single walled carbon nanotubes⁴⁶ and other photovoltaic materials.⁴⁷ This work has inspired the design of photovoltaics and other solar light harvesting devices to capitalize on the effective energy transfer that photosynthetic systems perform due to quantum coherence.^{29,48–50} Quantum coherence is not only prevalent in electronic systems, but it can be observed in vibrational modes with 2D IR as well.⁵ At a more fundamental level, the challenge for 2D spectroscopists and theorists in this

field is to relate the observed quantum coherence to function of the photosynthetic system itself. Overall, 2D ES has opened the door for a deeper understanding of energy transfer in nature to be applied to synthetic systems for more effective and efficient solar light harvesting.

TRANSPORT MECHANISMS IN ION CHANNELS

Ion channels are multimeric proteins responsible for initiating action potentials in neurons, muscle fibers, and other excitable cells through selective permeation of ions across the cell membrane.^{51–54} The mechanism of ion permeation and functional properties of ion channels have been thoroughly investigated with electrophysiological^{55,56} and spectroscopic^{57–59} techniques as well as molecular dynamics (MD) simulations.^{60–62} One of the most extensively studied are potassium (K^+) channels, which are the most diversely distributed, multifunctional ion channels found in nearly all living organisms. The KcsA potassium K^+ channel from *Streptomyces lividans* has often been used as a model system due to its small size and the fact that the sequence of its selectivity filter (⁷⁵TVGYG⁷⁹) is highly conserved among species.⁶³ The structure of KcsA and other channels has been resolved with X-ray crystallography,^{64–67} but the mechanism of ion conduction through the hydrophobic membrane has long been a matter of contention.^{60,68–73}

Two distinct mechanisms of ion conduction, commonly referred to as “knock-on” and “hard-knock” models, have been proposed. The structure of the KcsA ion channel and the two models are presented in Figure 3. In the “hard-knock” model, the conduction occurs solely due to strong repulsive interactions between K^+ ions that are found adjacent to one another in the selectivity filter.⁶⁹ In the “knock-on” model, the filter is occupied by two ions alternating with water molecules in a single file. As the third K^+ ion approaches the filter, the file shifts and one K^+ ion and one water molecule translocates across the membrane.

The critical evidence for the permeation mechanism had not been possible to obtain until recent advances in 2D optical spectroscopy. Kratochvil et al. used 2D IR spectroscopy on an isotope labeled semisynthetic KcsA channel to probe ion configurations, site-specific structure, and dynamics of the selectivity filter.⁷⁴ The isotope labels were introduced into three sites (Val,⁷⁶ Gly,⁷⁷ and Gly⁷⁹) to increase the sensitivity of 2D spectra to different ion configurations.^{74,75} The experimental 2D spectra and the spectra obtained from MD simulations are presented in parts A and B of Figure 3, respectively. The results show that the “knock-on” configurations are unquestionably more prevalent. Moreover, 2D line shape analysis indicates the presence of water molecules inside the filter, which is not consistent with the “hard-knock” model. Interestingly, 2D IR spectra showed the presence of a previously unresolved flipped state in which carbonyl groups on one of the monomeric units point outside of the filter. Such a flipped state had only been observed in MD simulations, and its biological function is not fully understood.

The same isotope labeling approach was used to study the structure of constricted states of KcsA with 2D IR spectroscopy.⁷⁶ At low K^+ concentration and at low pH, the selectivity filter collapses and no longer conducts ions. Moreover, at low pH, the helix bundle that comprises the intracellular gate undergoes a transition into an open state. It was found that,

despite the nearly identical structure of the selectivity filter, the ion occupancy differs between closed and open states, indicating a very complex conformational landscape of the KcsA channel.

2D IR spectroscopy of $^{13}\text{C}^{18}\text{O}$ isotope labels was also applied to studying pH-dependent solvation dynamics of the M2 proton channel from influenza A virus.^{77,78} At pH 6.2, when the M2 channel is in the open state, the isotopically labeled Gly34 senses bulk-like water molecules around its carbonyl group, as evidenced by fast spectral diffusion dynamics. In the closed state, at pH 8, water molecules become immobilized and are no longer able to form and break hydrogen bonds on a picosecond time scale. The study demonstrates the ability of 2D IR to probe water dynamics in complex protein environments.

Multidimensional spectroscopic techniques, including 2D IR, have only recently been applied to large biomolecular systems. Nonetheless, the 2D IR studies on KcsA show great promise that future studies will allow us to fully understand the mechanisms that govern the structure and functional properties of a variety of different ion channels.

CHEMICAL EXCHANGE DYNAMICS AND PERFORMANCE OF LITHIUM ION BATTERIES

Development of high energy density lithium ion batteries has been extensively researched due to their broad application in portable electronic devices, electric vehicles, and grid-scale energy storage.^{79–82} The primary components of lithium ion batteries are positive and negative electrodes and a liquid electrolyte. The electrolyte contains lithium salt such as lithium hexafluorophosphate (LiPF_6) dissolved in organic solvent.⁸³ Liquid carbonates are often used in a solvent mixture;⁸⁴ however, room temperature ionic liquids (RTILs) have been proposed as a safer alternative.^{85,86}

The electrochemical performance of Li ion batteries is strongly dependent on the type of electrolyte used, since intermolecular interactions between solvent and ions determine Li^+ ion mobility.⁸³ Thus, to design an efficient high energy density Li ion battery, one needs to understand both the solvation structure and solvation dynamics of the electrolyte mixture. 2D IR spectroscopy shows great promise for studying such phenomena because of its ability to observe chemical exchange dynamics^{87,88} between different solvation structures that occur on time scales as fast as picoseconds.

Recently, Lee and co-workers have studied exchange dynamics with 2D IR on electrolyte solution of lithium ions dissolved in diethyl carbonate (DEC).⁸⁹ In their study, the carbonyl stretch of DEC is used as a vibrational probe that senses the presence of Li^+ ion in its vicinity, giving rise to two separate peaks corresponding to free and Li-bound carbonate. It was found that $\text{Li}^+\cdots\text{DEC}$ complex forms within 17 ps and breaks with a time constant of only 2.2 ps at 1.0 M LiPF_6 concentration. The results imply that the mechanism of ion transport during the charging and discharging process in Li ion batteries might be strongly related to ultrafast solvent fluctuations and the time scales at which Li^+ forms a complex with the surrounding solvent molecules. It also suggests that existing theories on ion

diffusion in Li ion batteries may need to be reformulated with the aid of experimental data obtained from various 2D IR experiments.

Since the use of volatile and flammable solvents, such as DEC, can pose great safety concerns,⁸⁰ researchers have shown interest in room temperature ionic liquids (RTILs) as the solvent in liquid electrolytes.^{90,91} The Fayer group has introduced a number of chemically modified ionic liquids which incorporate vibrationally active probes.^{92–95} Those RTILs are used in conjunction with 2D IR spectroscopy and optical Kerr effect measurements to study orientational and spectral diffusion dynamics of ionic liquids in complex mixtures. The results provide a microscopic description of dynamics and intermolecular interactions in ionic liquid systems that may potentially find its use in the development of novel RTILs for Li ion batteries and other energy sources.

CHARGE TRANSFER EFFICIENCY IN PHOTOVOLTAIC MATERIALS

Across the globe, a major focus in research is to achieve an abundant, low cost energy solution. Significant efforts are aimed at improving and better understanding the factors governing photovoltaic efficiency.^{96,97} Electronic processes occurring on ultrafast time scales are at the heart of this topic. While transient absorption has provided many important insights into the underlying photophysics,^{98–101} 2D spectroscopy offers the unique advantage of spectrally resolving the excitation frequency, allowing for the responses of different excitation pathways to be separated.

2D ES shows great promise for understanding energetic delocalization, charge generation, and charge transfer processes in photovoltaics. Song and Scholes used 2D ES to map charge transfer pathways and demonstrate the role of hot electron transfer in poly(3-hexylthiophene) (P3HT) blends.⁵⁰ Vibrational coherence was shown to play a role in the process, transferring from the P3HT exciton to the P3HT polaron. 2D IR spectroscopy has been used to probe vibrational dynamics as a function of temperature in phenyl-C61-butyric acid methyl ester (PCBM), finding temperature independent dynamics,¹⁰² consistent with previous findings of temperature-independent rates of charge separation that suggested an activationless pathway.^{103,104} 2D photocurrent spectroscopy, which has been gaining popularity in the past few years,¹⁰⁵ has also recently been used to probe the ultrafast dynamics of photoexcitons into charge-producing states.¹⁰⁶

Singlet fission is currently a topic of immense interest with regard to the development of solar cells that can exceed the Shockley–Queisser efficiency limit.^{107,108} It occurs when a spin-singlet exciton converts to a pair of spin-triplet excitons localized on neighboring molecules. In principle, this process can increase the efficiency limit of a solar cell, but the underlying mechanism is not well understood. There has been significant debate in the literature concerning whether a direct coupling or charge transfer state-mediated mechanism is at work. Pentacene and its derivatives are among the most popular model systems for investigating singlet fission, as its triplet state lies at nearly half the energy of the lowest lying excited singlet state, resulting in some of the highest external quantum efficiencies reported to date.¹⁰⁹ Egorva and Rao used coherent 2D ES to explore the origin of the states involved in singlet fission of pentacene derivatives.¹¹⁰ Their work showed that vibrational

degrees of freedom couple the singlet and multiexciton state, which is optically dark and thus can only be populated via the singlet state, and mediate singlet fission.

Carbon nanotubes represent another promising material for harvesting light in solar cells. 2D ES has recently made significant advances in understanding their mechanisms of photoexcitation, energy redistribution, energy transfer, and exciton hopping.^{111–116} For example, Mehlenbacher and coworkers were able to map the pathways for energy flow in thin films of highly purified semiconducting nanotubes. Figure 4 summarizes some of these results for the S_1 states.¹¹⁴ While the S_2 exciton pathways depended on bandgap (not shown), the S_1 excitations relaxed independent of bandgap (Figure 4). These experiments have advanced our fundamental understanding of the photophysics and energy flow in carbon nanotubes, which will inform future attempts at designing carbon-nanotube-based solar cells.

UP AND COMING METHODS IN 2D SPECTROSCOPY

In the past two decades, 2D spectroscopy has clearly enabled important scientific discoveries in a broad range of scientific areas. To continue advancing our knowledge of structure and dynamics, new approaches and improvements to 2D methods are constantly in development.

Bredenbeck, Hamm, and Kraack have recently pioneered 2D IR spectroelectrochemistry in both solution¹¹⁷ and a surface-sensitive ATR geometry,¹¹⁸ which enables 2D IR spectra to be collected under controlled redox potentials. FTIR spectroelectrochemistry has a rich history studying electrode surface processes and redox chemistry, making the 2D implementation an exciting direction with great promise for better understanding structures and ultrafast dynamics of a variety of species, including interfacial solvent–electrode chemistry and redox proteins.

The Fayer lab recently reported a method for collecting 2D IR spectra in a “near-Brewster’s angle” reflective pump–probe geometry.³¹ This approach involves orienting the probe pulse, which serves as the local oscillator, close to the Brewster’s angle with respect to the sample surface, such that the local oscillator is strongly attenuated relative to the emitted signal. This results in large signal-to-noise enhancement, relative to the transmission geometry, enabling studies of thin films and monolayers that would otherwise be difficult to study.

2D IR microscopy has also recently been developed, providing spatially resolved 2D vibrational spectra in heterogeneous samples. Both point mapping¹¹⁹ and wide-field¹²⁰ implementations have been demonstrated. These methods hold great promise for studying a wide range of heterogeneous systems such as amyloid diseases in tissue, protein folding, and/or aggregation in heterogeneous environments, and material devices containing mid-IR vibrational reporters.

New laser technology also continues to expand the horizons of the field. Diode-pumped ytterbium (Yb) oscillators and amplifiers that operate at higher repetition rates show great promise for cost-effective ultrafast sources, which, when coupled with high efficiency OPAs and OPOs, can generate the wavelengths necessary for 2D ES and IR spectroscopies. The higher repetition rates allow for increased data acquisition rates and significantly improved

signal-to-noise. 100 kHz Yb laser systems are now in use for 2D spectroscopy at both visible¹²¹ and IR^{122,123} wavelengths.

A natural extension of 2D ES and 2D IR are 2D methods that bridge the two wavelength regimes. Khalil and co-workers have reported 2D experiments that combine the visible and IR wavelengths, allowing for vibrational–electronic couplings and vibronic processes, such as how vibrational motions mediate charge transfer and couple electronic states, to be monitored. Both IR-pump vis-probe^{124–126} and vis-pump IR-probe¹²⁷ have been reported. Though we have not focused on Raman spectroscopy here, 2D Raman-THz and^{128,129} 2D IR-Raman¹²⁶ spectroscopies have also been developed.

CONCLUSION

2D spectroscopy has the capability to measure biological, materials, and chemical systems in solid and solutions states, as well as at interfaces. The work presented here shows examples of the versatility of the technique for investigating the structure and dynamics of a variety of different chemical systems. 2D IR has provided insight on the mechanism of amyloid formation and ion-channel dynamics, and 2D ES has been used to monitor charge transfer in photosynthetic systems, carbon nanotubes, and other photovoltaics. While these are specific examples of how 2D spectroscopy can be used to probe structural and dynamic scientific questions, it is by no means an exhaustive list. As 2D spectroscopy becomes more accessible and ubiquitous, the number and types of systems studied can only increase. In the future, we believe 2D spectroscopy will continue to answer difficult core scientific questions in the fields of biology, materials science, and chemistry.

ACKNOWLEDGMENTS

We thank the members of the Zanni group for helpful discussions. J.P.L. is a Howard Hughes Medical Institute Fellow of the Life Sciences Research Foundation.

Funding

The writing of this Mini-Review Article and the research contained within it was supported by the NIH NIDDK 79895, NIH GM 102387, the NSF CHE 1665110, and the AFOSR FA9550–15-1–0061.

Biographies

Megan K. Petti was born in Idaho Falls, ID, and received her B.S. degree in Chemistry from the University of Notre Dame. She is currently a Ph.D. student in the lab of Prof. Martin T. Zanni at the University of Wisconsin–Madison. Her research focuses on developing new surface sensitive 2D IR techniques to measure biological interfaces.

Justin P. Lomont was born in Holland, MI. He received his B.S. in Chemistry from the University of Michigan under the supervision of Prof. Brian P. Coppola and his Ph.D. in Chemistry from the University of California–Berkeley under the direction of Prof. Charles B. Harris. He is currently a postdoctoral scholar in the lab of Prof. Martin T. Zanni at the University of Wisconsin–Madison and is a Howard Hughes Medical Institute fellow of the Life Sciences Research Foundation. His research is focused on understanding mechanisms of protein misfolding and aggregation in amyloid diseases.

Michał Maj was born in Luba, Poland. He received his B.Sc. in Chemistry from Wrocław University of Technology under the direction of Prof. Robert W. Gora and his Ph.D. from Korea University in Seoul, where he worked under the guidance of Prof. Minhaeng Cho. He is now researching under Prof. Martin T. Zanni at University of Wisconsin–Madison. His research focuses on studying the structure and aggregation propensities of human islet amyloid polypeptide with 2D IR spectroscopy.

Martin T. Zanni is the Meloche-Bascom Professor of Chemistry at the University of Wisconsin–Madison. He is one of the early innovators of 2D IR spectroscopy and has made many technological innovations in 2D IR, 2D visible, and 2D SFG spectroscopy that have broadened the capabilities and scope of multidimensional spectroscopies. He utilizes these new techniques to study topics in biophysics, chemical physics, photovoltaics, and surface science, for which he has received many national and international accolades for his research. He founded PhaseTech Spectroscopy Inc., which is the first company to commercialize 2D IR and 2D visible spectroscopies.

REFERENCES

- (1). Hamm P; Zanni MT Concepts and Methods of 2D Infrared Spectroscopy; Cambridge University Press: New York, 2011.
- (2). Cho M Two-Dimensional Optical Spectroscopy; Taylor & Francis Group: Boca Raton, FL, 2009.
- (3). Mukamel S Principles of Nonlinear Optical Spectroscopy; Oxford University Press: New York, 1995.
- (4). Ghosh A; Ostrander JS; Zanni MT Watching Proteins Wiggle: Mapping Structures with Two-Dimensional Infrared Spectroscopy. *Chem. Rev* 2017, 117(16), 10726–10759. [PubMed: 28060489]
- (5). Khalil M; Demirdöven N; Tokmakoff, a. Coherent 2D IR Spectroscopy: Molecular Structure and Dynamics in Solution. *J. Phys. Chem. A* 2003, 107 (27), 5258–5279.
- (6). Lomont JP; Ostrander JS; Ho J-J; Petti MK; Zanni MT Not All β -Sheets Are the Same: Amyloid Infrared Spectra, Transition Dipole Strengths, and Couplings Investigated by 2D IR Spectroscopy. *J. Phys. Chem. B* 2017, 121 (38), 8935–3845. [PubMed: 28851219]
- (7). Dunkelberger EB; Grechko M; Zanni MT Transition Dipoles from 1D and 2D Infrared Spectroscopy Help Reveal the Secondary Structures of Proteins: Application to Amyloids. *J. Phys. Chem. B* 2015, 119 (44), 14065–14075. [PubMed: 26446575]
- (8). Moran SD; Zanni MT How to Get Insight into Amyloid Structure and Formation from Infrared Spectroscopy. *J. Phys. Chem. Lett* 2014, 5 (11), 1984–1993. [PubMed: 24932380]
- (9). Demirdöven N; Cheatum CM; Chung HS; Khalil M; Knoester J; Tokmakoff A Two-Dimensional Infrared Spectroscopy of Antiparallel β -Sheet Secondary Structure. *J. Am. Chem. Soc* 2004, 126 (25), 7981–7990. [PubMed: 15212548]
- (10). Hahn S; Kim SS; Lee C; Cho M Characteristic Two-Dimensional IR Spectroscopic Features of Antiparallel and Parallel β -Sheet Polypeptides: Simulation Studies. *J. Chem. Phys* 2005, 123 (8), 084905. [PubMed: 16164328]
- (11). Wang L; Middleton CT; Singh S; Reddy AS; Woys AM; Strasfeld DB; Marek P; Raleigh DP; De Pablo JJ; Zanni MT; Skinner JL 2DIR Spectroscopy of Human Amylin Fibrils Reflects Stable β -Sheet Structure. *J. Am. Chem. Soc* 2011, 133 (40), 16062–16071. [PubMed: 21916515]
- (12). Luca S; Yau W-M; Leapman RD; Tycko R NIH Public Access. *Biochemistry* 2007, 46 (47), 13505–13522. [PubMed: 17979302]
- (13). Opie EL On the Relation of Chronic Interstitial Pancreatitis to the Island of Langerhans and to Diabetes Mellitus. *J. Exp. Med* 1901, 5 (4), 397–428. [PubMed: 19866952]
- (14). Opie EL The Relation of Diabetes Mellitus to Lesions of the Pancreas. Hyaline Degeneration of the Islands of Langerhans. *J. Exp. Med* 1901, 5 (5), 527–540. [PubMed: 19866956]

- (15). Shim S-H; Strasfeld DB; Ling YL; Zanni MT Automated 2D IR Spectroscopy Using a Mid-IR Pulse Shaper and Application of This Technology to the Human Islet Amyloid Polypeptide. *Proc. Natl. Acad. Sci. U. S. A* 2007, 104 (36), 14197–14202. [PubMed: 17502604]
- (16). Dunkelberger EB; Buchanan LE; Marek P; Cao P; Raleigh DP; Zanni MT Deamidation Accelerates Amyloid Formation and Alters Amylin Fiber Structure. *J. Am. Chem. Soc* 2012, 134 (30), 12658–12667. [PubMed: 22734583]
- (17). Strasfeld DB; Ling YL; Shim S; Zanni MT *J. Am. Chem. Soc* 2008, 130, 6698–6699. [PubMed: 18459774]
- (18). Buchanan LE; Dunkelberger EB; Tran HQ; Cheng P-NN; Chiu C-CC; Cao P; Raleigh DP; de Pablo JJ; Nowick JS; Zanni MT Mechanism of IAPP Amyloid Fibril Formation Involves an Intermediate with a Transient Beta-Sheet. *Proc. Natl. Acad. Sci. U. S.A* 2013, 110 (48), 19285–19290. [PubMed: 24218609]
- (19). Serrano AL; Lomont JP; Tu L-H; Raleigh DP; Zanni MT A Free Energy Barrier Caused by the Refolding of an Oligomeric Intermediate Controls the Lag Time of Amyloid Formation by HIAPP. *J. Am. Chem. Soc* 2017, 139 (46), 16748–16758. [PubMed: 29072444]
- (20). Maj M; Lomont JP; Rich KL; Alperstein AM; Zanni MT Site-Specific Detection of Protein Secondary Structure Using 2D IR Dihedral Indexing: A Proposed Assembly Mechanism of Oligomeric HIAPP. *Chem. Sci* 2018, 9, 463–474. [PubMed: 29619202]
- (21). Petkova AT; Ishii Y; Balbach JJ; Antzutkin ON; Leapman RD; Delaglio F; Tycko R A Structural Model for Alzheimer's β -Amyloid Fibrils Based on Experimental Constraints from Solid State NMR. *Proc. Natl. Acad. Sci. U. S. A* 2002, 99 (26), 16742–16747. [PubMed: 12481027]
- (22). Kim YS; Liu L; Axelsen PH; Hochstrasser RM Two-Dimensional Infrared Spectra of Isotopically Diluted Amyloid Fibrils from A β 40. *Proc. Natl. Acad. Sci. U. S. A* 2008, 105 (22), 7720–7725. [PubMed: 18499799]
- (23). Kim YS; Liu L; Axelsen PH; Hochstrasser RM 2D IR Provides Evidence for Mobile Water Molecules in β -Amyloid Fibrils. *Proc. Natl. Acad. Sci. U. S. A* 2009, 106 (42), 17751–17756. [PubMed: 19815514]
- (24). Zhuang W; Sgourakis NG; Li Z; Garcia AE; Mukamel S Discriminating Early Stage A β 42 Monomer Structures Using Chirality-Induced 2DIR Spectroscopy in a Simulation Study. *Proc. Natl. Acad. Sci. U. S. A* 2010, 107 (36), 15687–15692. [PubMed: 20798063]
- (25). Roeters SJ; Iyer A; Pletikapic G; Kogan V; Subramaniam V; Woutersen S Evidence for Intramolecular Antiparallel Beta-Sheet Structure in Alpha-Synuclein Fibrils from a Combination of Two-Dimensional Infrared Spectroscopy and Atomic Force Microscopy. *Sci. Rep* 2017, 7, 41051. [PubMed: 28112214]
- (26). Iyer A; Roeters SJ; Schilderink N; Hommersom B; Heeren RMA; Woutersen S; Claessens MMAE; Subramaniam XV The Impact of N-Terminal Acetylation of α -Synuclein on Phospholipid Membrane Binding and Fibril Structure. *J. Biol. Chem* 2016, 291 (40), 21110–21122. [PubMed: 27531743]
- (27). Buchanan LE; Carr JK; Fluijt AM; Hoganson AJ; Moran SD; Pablo JJ De. Structural Motif of Polyglutamine Amyloid Fibrils Discerned with Mixed-Isotope Infrared Spectroscopy. *Proc. Natl. Acad. Sci. U. S. A* 2014, 111 (16), 5796–5801. [PubMed: 24550484]
- (28). Zhang TO; Alperstein AM; Zanni MT Amyloid β -Sheet Secondary Structure Identified in UV-Induced Cataracts of Porcine Lenses Using 2D IR Spectroscopy. *J. Mol. Biol* 2017, 429 (11), 1705–1721. [PubMed: 28454743]
- (29). Bredas J-L; Sargent EH; Scholes GD Photovoltaic Concepts Inspired by Coherence Effects in Photosynthetic Systems. *Nat. Mater* 2017, 16 (1), 35–44.
- (30). Scholes GD; Fleming GR; Chen LX; Aspuru-Guzik A; Buchleitner A; Coker DF; Engel GS; van Grondelle R; Ishizaki A; Jonas DM; et al. Using Coherence to Enhance Function in Chemical and Biophysical Systems. *Nature* 2017, 543 (7647), 647–656. [PubMed: 28358065]
- (31). Nishida J; Yan C; Fayer MD Enhanced Nonlinear Spectroscopy for Monolayers and Thin Films in Near-Brewster's Angle Reflection Pump-Probe Geometry. *J. Chem. Phys* 2017, 146 (9), 094201.

- (32). Pislakov AV; Mancal T; Fleming GR Two-Dimensional Optical Three-Pulse Photon Echo Spectroscopy. II. Signatures of Coherent Electronic Motion and Exciton Population Transfer in Dimer Two-Dimensional Spectra. *J. Chem. Phys* 2006, 124 (23), 234505. [PubMed: 16821927]
- (33). Sundström V; Pullerits T; van Grondelle R Photosynthetic Light-Harvesting: Reconciling Dynamics and Structure of Purple Bacterial LH2 Reveals Function of Photosynthetic Unit. *J. Phys. Chem. B* 1999, 103 (13), 2327–2346.
- (34). Scholes GD; Fleming GR On the Mechanism of Light Harvesting in Photosynthetic Purple Bacteria: B800 to B850 Energy Transfer. *J. Phys. Chem. B* 2000, 104 (8), 1854–1868.
- (35). Scholes GD; Fleming GR; Olaya-Castro A; van Grondelle R Lessons from Nature about Solar Light Harvesting. *Nat. Chem* 2011, 3 (10), 763–774. [PubMed: 21941248]
- (36). Engel GS; Calhoun TR; Read EL; Ahn T-K; Mancal T; Cheng Y-C; Blankenship RE; Fleming GR Evidence for Wavelike Energy Transfer through Quantum Coherence in Photo-synthetic Systems. *Nature* 2007, 446 (7137), 782–786. [PubMed: 17429397]
- (37). Brixner T; Stenger J; Vaswani HM; Cho M; Blankenship RE; Fleming GR Two-Dimensional Spectroscopy of Electronic Couplings in Photosynthesis. *Nature* 2005, 434 (7033), 625–628. [PubMed: 15800619]
- (38). Lee H; Cheng Y-C; Fleming GR Coherence Dynamics in Photosynthesis: Protein Protection of Excitonic Coherence. *Science* 2007, 316 (5830), 1462–1465. [PubMed: 17556580]
- (39). Wang C; Flanagan ML; McGillicuddy RD; Zheng H; Ginzburg AR; Yang X; Moffat K; Engel GS Bacteriophyto-chrome Photoisomerization Proceeds Homogeneously Despite Heterogeneity in Ground State. *Biophys. J* 2016, 111 (10), 2125–2134. [PubMed: 27851937]
- (40). Fuller FD; Pan J; Gelzinis A; Butkus V; Senlik SS; Wilcox DE; Yocum CF; Valkunas L; Abramavicius D; Ogilvie JP Vibronic Coherence in Oxygenic Photosynthesis. *Nat. Chem* 2014, 6 (8), 706–711. [PubMed: 25054941]
- (41). Duan H-G; Prokhorenko VI; Cogdell R; Ashraf K; Stevens AL; Thorwart M; Miller RJD Nature Does Not Rely on Long-Lived Electronic Quantum Coherence for Photosynthetic Energy Transfer. *Proc. Natl. Acad. Sci. U. S. A* 2017, 114 (32), 8493–8498. [PubMed: 28743751]
- (42). Dostál J; Pšeník J; Zigmantas D In Situ Mapping of the Energy Flow through the Entire Photosynthetic Apparatus. *Nat. Chem* 2016, 8 (7), 705–710. [PubMed: 27325098]
- (43). Tempelaar R; Halpin A; Johnson PJM; Cai J; Murphy RS; Knoester J; Miller RJD; Jansen TLC Laser-Limited Signatures of Quantum Coherence. *J. Phys. Chem. A* 2016, 120 (19), 3042–3048. [PubMed: 26558888]
- (44). Butkus V; Dong H; Fleming GR; Abramavicius D; Valkunas L Disorder-Induced Quantum Beats in Two-Dimensional Spectra of Excitonically Coupled Molecules. *J. Phys. Chem. Lett* 2016, 7 (2), 277–282. [PubMed: 26720834]
- (45). Zhang Z; Wang J Assistance of Molecular Vibrations on Coherent Energy Transfer in Photosynthesis from the View of a Quantum Heat Engine. *J. Phys. Chem. B* 2015, 119 (13), 4662–4667. [PubMed: 25776946]
- (46). Wang L; Griffin GB; Zhang A; Zhai F; Williams NE; Jordan RF; Engel GS Controlling Quantum-Beating Signals in 2D Electronic Spectra by Packing Synthetic Heterodimers on Single-Walled Carbon Nanotubes. *Nat. Chem* 2017, 9 (3), 219–225. [PubMed: 28221350]
- (47). Falke SM; Rozzi CA; Brida D; Maiuri M; Amato M; Sommer E; De Sio A; Rubio A; Cerullo G; Molinari E; Lienau C Coherent Ultrafast Charge Transfer in an Organic Photovoltaic Blend. *Science* 2014, 344 (6187), 1001–1005. [PubMed: 24876491]
- (48). Collini E; Scholes GD Coherent Intrachain Energy Migration in a Conjugated Polymer at Room Temperature. *Science* 2009, 323 (5912), 369–373. [PubMed: 19150843]
- (49). Tamura H; Martinazzo R; Ruckebauer M; Burghardt I Quantum Dynamics of Ultrafast Charge Transfer at an Oligothiophene-Fullerene Heterojunction. *J. Chem. Phys* 2012, 137 (22), 22A540.
- (50). Song Y; Clifton SN; Pensack RD; Kee TW; Scholes GD Vibrational Coherence Probes the Mechanism of Ultrafast Electron Transfer in Polymer–fullerene Blends. *Nat. Commun* 2014, 5, 4933. [PubMed: 25215959]
- (51). Kurachi Y; North A Ion Channels: Their Structure, Function and Control – an Overview. *J. Physiol* 2004, 554 (2), 245–247.

- (52). Sachs F Mechanical Transduction by Membrane Ion Channels: A Mini Review. *Mol. Cell. Biochem* 1991, 104 (1–2), 57–60. [PubMed: 1717821]
- (53). Hille B *Ionic Channels of Excitable Membranes*; Sinauer: Sunderland, MA, 2001.
- (54). Catterall WA Structure and Function of Voltage-Gated Ion Channels. *Annu. Rev. Biochem* 1995, 64 (1), 493–531. [PubMed: 7574491]
- (55). Morais-Cabral JH; Zhou Y; MacKinnon R Energetic Optimization of Ion Conduction Rate by the K⁺ Selectivity Filter. *Nature* 2001, 414 (6859), 37–42. [PubMed: 11689935]
- (56). Dunlop J; Bowlby M; Peri R; Vasilyev D; Arias R High-Throughput Electrophysiology: An Emerging Paradigm for Ion-Channel Screening and Physiology. *Nat. Rev. Drug Discovery* 2008, 7(4), 358–368. [PubMed: 18356919]
- (57). Cha A; Snyder GE; Selvin PR; Bezanilla F Atomic Scale Movement of the Voltage-Sensing Region in a Potassium Channel Measured via Spectroscopy. *Nature* 1999, 402 (6763), 809–813. [PubMed: 10617201]
- (58). Stevenson P; Götz C; Baiz CR; Akerboom J; Tokmakoff A; Vaziri A Visualizing KcsA Conformational Changes upon Ion Binding by Infrared Spectroscopy and Atomistic Modeling. *J. Phys. Chem. B* 2015, 119 (18), 5824–5831. [PubMed: 25861001]
- (59). Perozo E; Cortes DM; Cuello LG Three-Dimensional Architecture and Gating Mechanism of a K⁺ Channel Studied by EPR Spectroscopy. *Nat. Struct. Biol* 1998, 5 (6), 459–469. [PubMed: 9628484]
- (60). Bernèche S; Roux B Energetics of Ion Conduction through the K⁺ Channel. *Nature* 2001, 414 (6859), 73–77. [PubMed: 11689945]
- (61). Cordero-Morales JF; Cuello LG; Zhao Y; Jogini V; Cortes DM; Roux B; Perozo E Molecular Determinants of Gating at the Potassium-Channel Selectivity Filter. *Nat. Struct. Mol. Biol* 2006, 13 (4), 311–318. [PubMed: 16532009]
- (62). Noskov SY; Bernèche S; Roux B Control of Ion Selectivity in Potassium Channels by Electrostatic and Dynamic Properties of Carbonyl Ligands. *Nature* 2004, 431 (7010), 830–834. [PubMed: 15483608]
- (63). MacKinnon R; Cohen SL; Kuo A; Lee A; Chait BT Structural Conservation in Prokaryotic and Eukaryotic Potassium Channels. *Science* 1998, 280 (5360), 106–109. [PubMed: 9525854]
- (64). Payandeh J; Scheuer T; Zheng N; Catterall WA The Crystal Structure of a Voltage-Gated Sodium Channel. *Nature* 2011, 475 (7356), 353–358. [PubMed: 21743477]
- (65). Sula A; Booker J; Ng LCT; Naylor CE; DeCaen PG; Wallace BA The Complete Structure of an Activated Open Sodium Channel. *Nat. Commun* 2017, 8, 14205. [PubMed: 28205548]
- (66). Jiang Y; Lee A; Chen J; Ruta V; Cadene M; Chait BT; MacKinnon R X-Ray Structure of a Voltage-Dependent K⁺ Channel. *Nature* 2003, 423 (6935), 33–41. [PubMed: 12721618]
- (67). Uysal S; Vázquez V; Tereshko V; Esaki K; Fellouse FA; Sidhu SS; Koide S; Perozo E; Kossiakov A Crystal Structure of Full-Length KcsA in Its Closed Conformation. *Proc. Natl. Acad. Sci. U.S.A* 2009, 106 (16), 6644–6649. [PubMed: 19346472]
- (68). Nelson PH A Permeation Theory for Single-File Ion Channels: One- and Two-Step Models. *J. Chem. Phys* 2011, 134 (16), 165102. [PubMed: 21528981]
- (69). Köpfer DA; Song C; Gruene T; Sheldrick GM; Zachariae U; Groot BL de. Ion Permeation in K⁺ Channels Occurs by Direct Coulomb Knock-On. *Science* 2014, 346 (6207), 352–355. [PubMed: 25324389]
- (70). Hummer G Potassium Ions Line Up. *Science* 2014, 346 (6207), 303–303. [PubMed: 25324373]
- (71). Åqvist J; Luzhkov V Ion Permeation Mechanism of the Potassium Channel. *Nature* 2000, 404 (6780), 881–884. [PubMed: 10786795]
- (72). Doyle DA; Morais Cabral J; Pfuetzner RA; Kuo A; Gulbis JM; Cohen SL; Chait BT; MacKinnon R The Structure of the Potassium Channel: Molecular Basis of K⁺ Conduction and Selectivity. *Science* 1998, 280 (5360), 69–77. [PubMed: 9525859]
- (73). Zhou Y; MacKinnon R The Occupancy of Ions in the K⁺ Selectivity Filter: Charge Balance and Coupling of Ion Binding to a Protein Conformational Change Underlie High Conduction Rates. *J. Mol. Biol* 2003, 333 (5), 965–975. [PubMed: 14583193]

- (74). Kratochvil HT; Carr JK; Matulef K; Annen AW; Li H; Maj M; Ostmeier J; Serrano AL; Raghuraman H; Moran SD; et al. Instantaneous Ion Configurations in the K⁺ Ion Channel Selectivity Filter Revealed by 2D IR Spectroscopy. *Science* 2016, 353 (6303), 1040–1044. [PubMed: 27701114]
- (75). Ganim Z; Tokmakoff A; Vaziri A Vibrational Excitons in Ionophores: Experimental Probes for Quantum Coherence-Assisted Ion Transport and Selectivity in Ion Channels. *New J. Phys* 2011, 13(11), 113030.
- (76). Kratochvil HT; Maj M; Matulef K; Annen AW; Ostmeier J; Perozo E; Roux B; Valiyaveetil FI; Zanni MT Probing the Effects of Gating on the Ion Occupancy of the K⁺ Channel Selectivity Filter Using Two-Dimensional Infrared Spectroscopy. *J. Am. Chem. Soc* 2017, 139 (26), 8837–8845. [PubMed: 28472884]
- (77). Manor J; Mukherjee P; Lin Y-S; Leonov H; Skinner JL; Zanni MT; Arkin IT Gating Mechanism of the Influenza A M2 Channel Revealed by 1D and 2D IR Spectroscopies. *Structure* 2009, 17(2), 247–254. [PubMed: 19217395]
- (78). Ghosh A; Qiu J; DeGrado WF; Hochstrasser RM Tidal Surge in the M2 Proton Channel, Sensed by 2D IR Spectroscopy. *Proc. Natl. Acad. Sci. U. S. A* 2011, 108 (15), 6115–6120. [PubMed: 21444789]
- (79). Tarascon J-M; Armand M Issues and Challenges Facing Rechargeable Lithium Batteries. *Nature* 2001, 414 (6861), 359–367. [PubMed: 11713543]
- (80). Etacheri V; Marom R; Elazari R; Salitra G; Aurbach D Challenges in the Development of Advanced Li-Ion Batteries: A Review. *Energy Environ. Sci* 2011, 4 (9), 3243–3262.
- (81). Scrosati B; Garche J Lithium Batteries: Status, Prospects and Future. *J. Power Sources* 2010, 195 (9), 2419–2430.
- (82). Yoshino A Development of Lithium Ion Battery. *Mol. Cryst. Liq. Cryst. Sci. Technol., Sect. A* 2000, 340 (1), 425–429.
- (83). Aurbach D; Talyosef Y; Markovsky B; Markevich E; Zinigrad E; Asraf L; Gnanaraj JS; Kim H-J Design of Electrolyte Solutions for Li and Li-Ion Batteries: A Review. *Electrochim. Acta* 2004, 50 (2), 247–254.
- (84). Valøen LO; Reimers JN Transport Properties of LiPF₆-Based Li-Ion Battery Electrolytes. *J. Electrochem. Soc* 2005, 152 (5), A882–A891.
- (85). Gali ki M; Lewandowski A; St pniak I Ionic Liquids as Electrolytes. *Electrochim. Acta* 2006, 51 (26), 5567–5580.
- (86). Lewandowski A; widerska-Mocek, A. Ionic Liquids as Electrolytes for Li-Ion Batteries—An Overview of Electrochemical Studies. *J. Power Sources* 2009, 194 (2), 601–609.
- (87). Kim YS; Hochstrasser RM Chemical Exchange 2D IR of Hydrogen-Bond Making and Breaking. *Proc. Natl. Acad. Sci. U. S. A* 2005, 102 (32), 11185–11190. [PubMed: 16040800]
- (88). Zheng J; Kwak K; Asbury J; Chen X; Piletic IR; Fayer MD Ultrafast Dynamics of Solute-Solvent Complexation Observed at Thermal Equilibrium in Real Time. *Science* 2005, 309 (5739), 1338–1343. [PubMed: 16081697]
- (89). Lee K-K; Park K; Lee H; Noh Y; Kossowska D; Kwak K; Cho M Ultrafast Fluxional Exchange Dynamics in Electrolyte Solvation Sheath of Lithium Ion Battery. *Nat. Commun* 2017, 8, 14658. [PubMed: 28272396]
- (90). Guerfi A; Dontigny M; Charest P; Petitclerc M; Lagace M; Vijn A; Zaghbi K Improved Electrolytes for Li-Ion Batteries: Mixtures of Ionic Liquid and Organic Electrolyte with Enhanced Safety and Electrochemical Performance. *J. Power Sources* 2010, 195(3), 845–852.
- (91). Kühnel R-S; Böckenfeld N; Passerini S; Winter M; Balducci A Mixtures of Ionic Liquid and Organic Carbonate as Electrolyte with Improved Safety and Performance for Rechargeable Lithium Batteries. *Electrochim. Acta* 2011, 56 (11), 4092–4099.
- (92). Shin JY; Yamada SA; Fayer MD Dynamics of a Room Temperature Ionic Liquid in Supported Ionic Liquid Membranes vs the Bulk Liquid: 2D IR and Polarized IR Pump–Probe Experiments. *J. Am. Chem. Soc* 2017, 139 (1), 311–323. [PubMed: 27973786]
- (93). Nicolau BG; Sturlaugson A; Fruchey K; Ribeiro MCC; Fayer MD Room Temperature Ionic Liquid–Lithium Salt Mixtures: Optical Kerr Effect Dynamical Measurements. *J. Phys. Chem. B* 2010, 114 (25), 8350–8356. [PubMed: 20527943]

- (94). Lawler C; Fayer MD The Influence of Lithium Cations on Dynamics and Structure of Room Temperature Ionic Liquids. *J. Phys. Chem. B* 2013, 117 (33), 9768–9774. [PubMed: 23879633]
- (95). Yamada SA; Bailey HE; Tamimi A; Li C; Fayer MD Dynamics in a Room-Temperature Ionic Liquid from the Cation Perspective: 2D IR Vibrational Echo Spectroscopy. *J. Am. Chem. Soc* 2017, 139 (6), 2408–2420. [PubMed: 28099808]
- (96). Green MA Commercial Progress and Challenges for Photovoltaics. *Nat. Energy* 2016, 1 (1), 15015.
- (97). Green MA; Bremner SP Energy Conversion Approaches and Materials for High-Efficiency Photovoltaics. *Nat. Mater* 2017, 16(1), 23.
- (98). Walker BJ; Musser AJ; Beljonne D; Friend RH Singlet Exciton Fission in Solution. *Nat. Chem* 2013, 5 (12), 1019–1024. [PubMed: 24256865]
- (99). Yost SR; Lee J; Wilson MWB; Wu T; McMahon DP; Parkhurst RR; Thompson NJ; Congreve DN; Rao A; Johnson K; et al. Transferable Model for Singlet-Fission Kinetics. *Nat. Chem* 2014, 6 (6), 492. [PubMed: 24848234]
- (100). Lane PA; Cunningham PD; Melinger JS; Esenturk O; Heilweil EJ Hot Photocarrier Dynamics in Organic Solar Cells. *Nat. Commun* 2015, 6, 7558. [PubMed: 26179323]
- (101). Musser AJ; Liebel M; Schnedermann C; Wende T; Kehoe TB; Rao A; Kukura P Evidence for Conical Intersection Dynamics Mediating Ultrafast Singlet Exciton Fission. *Nat. Phys* 2015, 11 (4), 352.
- (102). Pensack RD; Banyas KM; Asbury JB Temperature-Independent Vibrational Dynamics in an Organic Photovoltaic Material. *J. Phys. Chem. B* 2010, 114 (38), 12242–12251. [PubMed: 20812710]
- (103). Pensack RD; Asbury JB Barrierless Free Carrier Formation in an Organic Photovoltaic Material Measured with Ultrafast Vibrational Spectroscopy. *J. Am. Chem. Soc* 2009, 131 (44), 15986–15987. [PubMed: 19886692]
- (104). Pensack RD; Asbury JB Beyond the Adiabatic Limit: Charge Photogeneration in Organic Photovoltaic Materials. *J. Phys. Chem. Lett* 2010, 1 (15), 2255–2263.
- (105). Bakulin AA; Silva C; Vella E Ultrafast Spectroscopy with Photocurrent Detection: Watching Excitonic Optoelectronic Systems at Work. *J. Phys. Chem. Lett* 2016, 7 (2), 250–258. [PubMed: 26711855]
- (106). Vella E; Li H; Grégoire P; Tuladhar SM; Vezie MS; Few S; Bazán CM; Nelson J; Silva-Acuña C; Bittner ER Ultrafast Decoherence Dynamics Govern Photocarrier Generation Efficiencies in Polymer Solar Cells. *Sci. Rep* 2016, 6, srep29437.
- (107). Shockley W; Queisser HJ Detailed Balance Limit of Efficiency of P-n Junction Solar Cells. *J. Appl. Phys* 1961, 32 (3), 510–519.
- (108). Smith MB; Michl J Singlet Fission. *Chem. Rev* 2010, 110(11), 6891–6936. [PubMed: 21053979]
- (109). Congreve DN; Lee J; Thompson NJ; Hontz E; Yost SR; Reuswig PD; Bahlke ME; Reineke S; Voorhis TV; Baldo MA External Quantum Efficiency Above 100% in a Singlet-Exciton-Fission-Based Organic Photovoltaic Cell. *Science* 2013, 340 (6130), 334–337. [PubMed: 23599489]
- (110). Bakulin AA; Morgan SE; Kehoe TB; Wilson MWB; Chin AW; Zigmantas D; Egorova D; Rao A Real-Time Observation of Multiexcitonic States in Ultrafast Singlet Fission Using Coherent 2D Electronic Spectroscopy. *Nat. Chem* 2016, 8 (1), 16–23. [PubMed: 26673260]
- (111). Mehlenbacher RD; Wu M-Y; Grechko M; Laaser JE; Arnold MS; Zanni MT Photoexcitation Dynamics of Coupled Semiconducting Carbon Nanotube Thin Films. *Nano Lett* 2013, 13(4), 1495–1501. [PubMed: 23464618]
- (112). Shea MJ; Mehlenbacher RD; Zanni MT; Arnold MS Experimental Measurement of the Binding Configuration and Coverage of Chirality-Sorting Polyfluorenes on Carbon Nanotubes. *J. Phys. Chem. Lett* 2014, 5 (21), 3742–3749. [PubMed: 26278744]
- (113). Grechko M; Ye Y; Mehlenbacher RD; McDonough TJ; Wu M-Y; Jacobberger RM; Arnold MS; Zanni MT Diffusion-Assisted Photoexcitation Transfer in Coupled Semiconducting Carbon Nanotube Thin Films. *ACS Nano* 2014, 8 (6), 5383–5394. [PubMed: 24806792]

- (114). Mehlenbacher RD; McDonough TJ; Grechko M; Wu M-Y; Arnold MS; Zanni MT Energy Transfer Pathways in Semiconducting Carbon Nanotubes Revealed Using Two-Dimensional White-Light Spectroscopy. *Nat. Commun* 2015, 6, 6732. [PubMed: 25865487]
- (115). Mehlenbacher RD; Wang J; Kearns NM; Shea MJ; Flach JT; McDonough TJ; Wu M-Y; Arnold MS; Zanni MT Ultrafast Exciton Hopping Observed in Bare Semiconducting Carbon Nanotube Thin Films with Two-Dimensional White-Light Spectroscopy. *J. Phys. Chem. Lett* 2016, 7 (11), 2024–2031. [PubMed: 27182690]
- (116). Mehlenbacher RD; McDonough TJ; Kearns NM; Shea MJ; Joo Y; Gopalan P; Arnold MS; Zanni MT Polarization-Controlled Two-Dimensional White-Light Spectroscopy of Semiconducting Carbon Nanotube Thin Films. *J. Phys. Chem. C* 2016, 120(30), 17069–17080.
- (117). El Khoury Y; Van Wilderen LJGW; Bredenbeck J Ultrafast 2D-IR Spectroelectrochemistry of Flavin Mononucleotide. *J. Chem. Phys* 2015, 142 (21), 212416. [PubMed: 26049436]
- (118). Lotti D; Hamm P; Kraack JP Surface-Sensitive Spectro-Electrochemistry Using Ultrafast 2D ATR IR Spectroscopy. *J. Phys. Chem. C* 2016, 120 (5), 2883–2892.
- (119). Baiz CR; Schach D; Tokmakoff A Ultrafast 2D IR Microscopy. *Opt. Express* 2014, 22 (15), 18724–18735. [PubMed: 25089490]
- (120). Ostrander JS; Serrano AL; Ghosh A; Zanni MT Spatially Resolved Two-Dimensional Infrared Spectroscopy via Wide-Field Microscopy. *ACS Photonics* 2016, 3 (7), 1315–1323. [PubMed: 27517058]
- (121). Kearns NM; Mehlenbacher RD; Jones AC; Zanni MT Broadband 2D Electronic Spectrometer Using White Light and Pulse Shaping: Noise and Signal Evaluation at 1 and 100 kHz. *Opt. Express* 2017, 25 (7), 7869–7883. [PubMed: 28380905]
- (122). Luther BM; Tracy KM; Gerrity M; Brown S; Krummel AT 2D IR Spectroscopy at 100 kHz Utilizing a Mid-IR OPCPA Laser Source. *Opt. Express* 2016, 24 (4), 4117. [PubMed: 26907062]
- (123). Greetham GM; Donaldson PM; Nation C; Sazanovich IV; Clark IP; Shaw DJ; Parker AW; Towrie MA 100 kHz Time-Resolved Multiple-Probe Femtosecond to Second Infrared Absorption Spectrometer. *Appl. Spectrosc* 2016, 70 (4), 645–653. [PubMed: 26887988]
- (124). Courtney TL; Fox ZW; Estergreen L; Khalil M Measuring Coherently Coupled Intramolecular Vibrational and Charge-Transfer Dynamics with Two-Dimensional Vibrational– Electronic Spectroscopy. *J. Phys. Chem. Lett* 2015, 6 (7), 1286–1292. [PubMed: 26262989]
- (125). Courtney TL; Fox ZW; Slenkamp KM; Khalil M Two-Dimensional Vibrational-Electronic Spectroscopy. *J. Chem. Phys* 2015, 143 (15), 154201. [PubMed: 26493900]
- (126). Courtney TL; Fox ZW; Slenkamp KM; Lynch MS; Khalil M Two-Dimensional Fourier Transform Infrared-Visible and Infrared-Raman Spectroscopies Ultrafast Phenomena XIX; Springer Proceedings in Physics; Springer: Cham, Switzerland, 2015; pp 503– 505.
- (127). Gaynor JD; Courtney TL; Balasubramanian M; Khalil M Fourier Transform Two-Dimensional Electronic-Vibrational Spectroscopy Using an Octave-Spanning Mid-IR Probe. *Opt. Lett* 2016, 41(12), 2895–2898. [PubMed: 27304316]
- (128). Hamm P 2D-Raman-THz Spectroscopy: A Sensitive Test of Polarizable Water Models. *J. Chem. Phys* 2014, 141 (18), 184201. [PubMed: 25399140]
- (129). Shalit A; Ahmed S; Savolainen J; Hamm P Terahertz Echoes Reveal the Inhomogeneity of Aqueous Salt Solutions. *Nat. Chem* 2017, 9 (3), 273–278. [PubMed: 28221356]

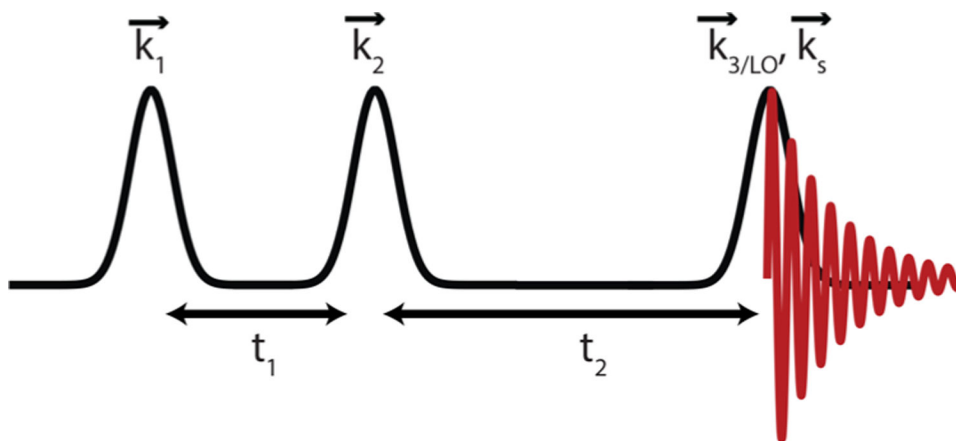


Figure 1. Pulse sequence used in a four-wave mixing experiment to obtain a two-dimensional infrared or electronic spectrum. Three field interactions with the sample produce an emitted signal that is heterodyned with either a local oscillator or the third laser pulse, depending on the experimental geometry.

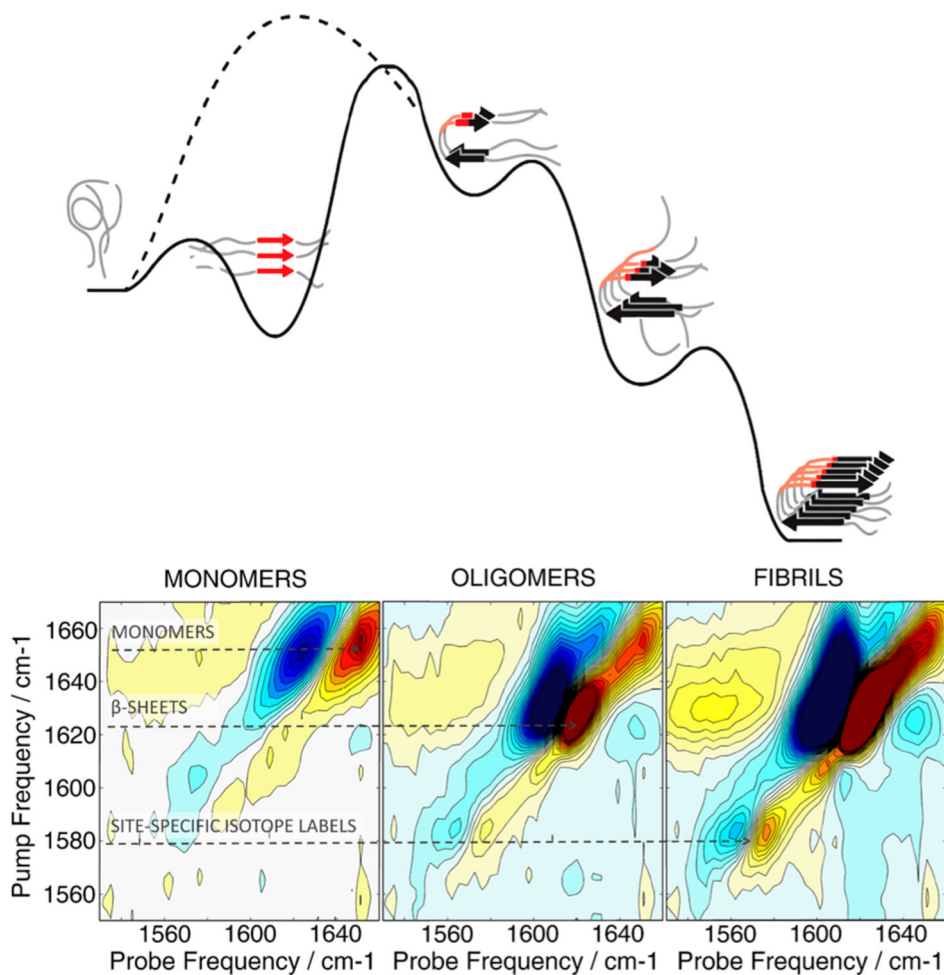


Figure 2. Top: Schematic free energy diagram of the multistep hIAPP aggregation process. The FGAIL region that participates in the formation of a transient β -sheet intermediate is highlighted in red. Introduction of a proline mutation into the FGAIL sequence inhibits aggregation by destabilizing the intermediate (dashed line). Bottom: 2D IR spectra of isotopically labeled (V17) hIAPP measured at different aggregation times are presented below. Dashed arrows show pump frequencies of 2D IR peaks originating from monomers, β -sheet aggregates, and site-specific isotope labels. Adapted with permission from ref 18.

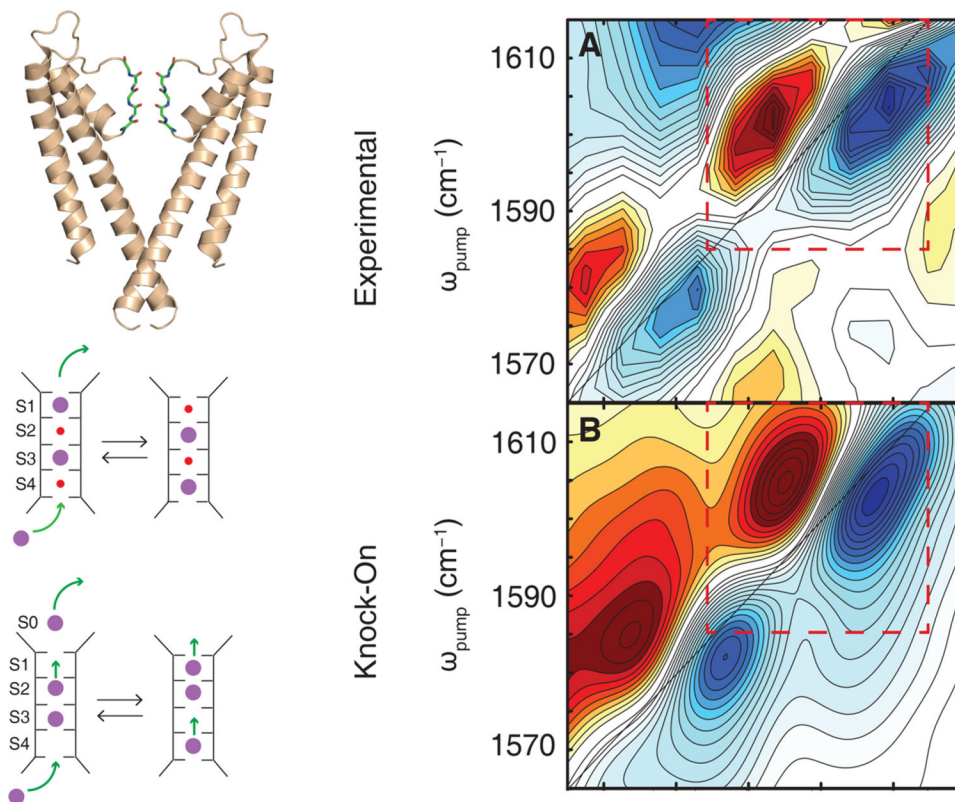


Figure 3. Left: The KcsA potassium ion channel and a schematic of the knock-on (top) and hard-knock (bottom) ion transport mechanisms. Right:(a) The experimental IR spectrum in the isotope labeled region and (b) the simulated 2D IR spectrum of the knock-on model. Reproduced with permission from refs 4 and 74. Copyright 2017 American Chemical Society and 2016 American Association for the Advancement of Science, respectively.

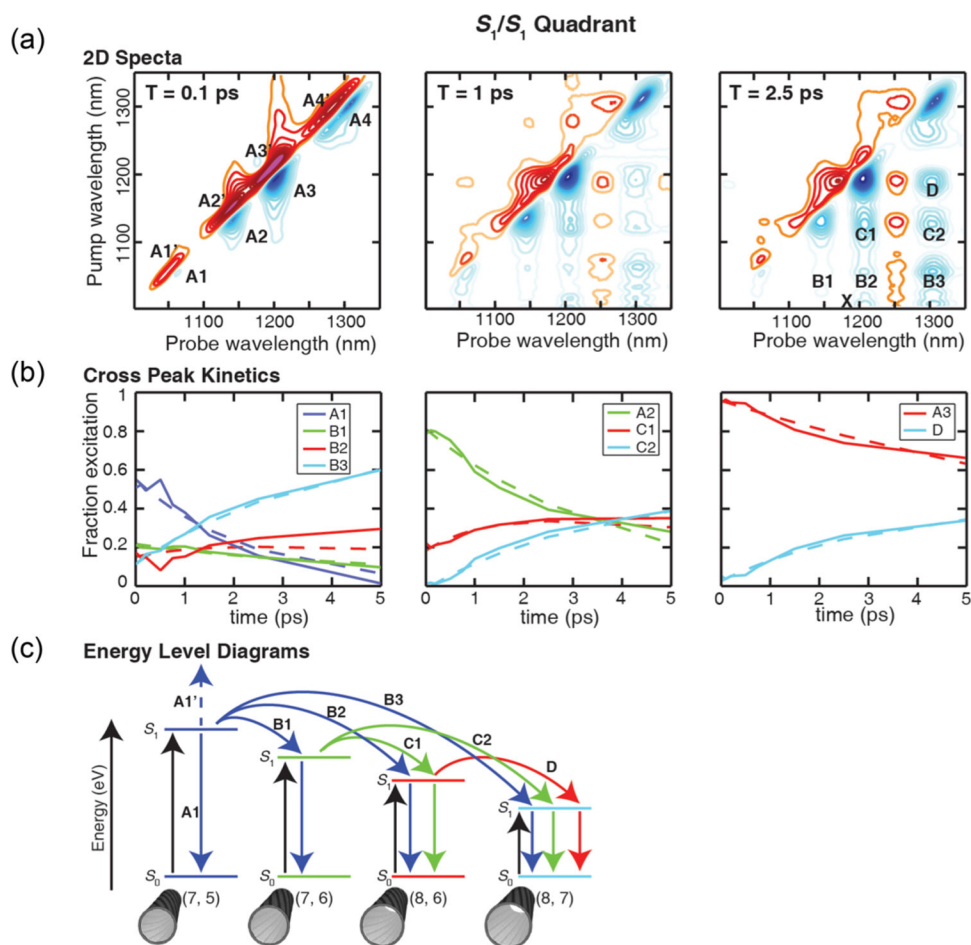


Figure 4. (a) 2D electronic spectra for the indicated pump–probe delays in the S₁/S₁ quadrant. The simultaneous growth of round cross-peaks indicates energy transfer is uncorrelated and independent of bandgap for S₁ excitons. (b) The kinetics of cross-peaks provide rates of energy transfer. Dashed lines are exponential fits to the data, and the measured time constants are all equal to within 1 ps. (c) An energy level diagram showing the energy transfer pathway for each peak in the 2D spectrum. Black arrows denote pumped transitions, while blue, green, and red arrows correspond to excitons initially excited on (7, 5), (7, 6), and (8, 6) nanotubes, respectively. Dashed arrows represent excited state absorption, solid arrows represent ground state bleaches/stimulated emission, and curved arrows denote energy transfer. Reproduced with permission from ref 114.